Work Functions of Functionalized Single-Walled Carbon Nanotubes

by

Janet Ryu

SUBMITTED TO THE DEPARTMENT OF
MATERIALS SCIENCE AND ENGINEERING IN PARTIAL
FULFILLMENT OF THE REQUIREMENTS FOR THE
DEGREE OF

BACHELORS OF SCIENCE IN MATERIALS SCIENCE AND ENGINEERING

AT THE

MASSACHUSETTS INSTITUTE OF TECHNOLOGY

[June 2006]

MAY 2006
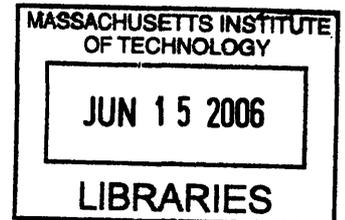
Signature of Author: ....
Department of Materials Science and Engineering
May 26, 2006

Certified by: ....
Nicola Marzari
Professor of Materials Science and Engineering
Thesis Supervisor

Accepted by: ....
Caroline Ross
Professor of Materials Science and Engineering
Chairman, Committee for Undergraduate Students

1

Work Functions of Functionalized Single-Walled Carbon Nanotubes

Janet S. Ryu

May 26, 2006

Contents

List of Tables

List of Figures

4

Chapter 1

Introduction

1.1 Carbon nanotubes

Carbon nanotube (CNT) structures were discovered by Sumio Iijima in 1991 at NEC laboratories in Japan. Since their discovery, scientists and engineers have been fascinated by their electrical and mechanical properties. Their unique characteristics, in addition to their nanoscale size, have generated much excitement about the possible applications of this novel material.

This excitement surrounding carbon nanotubes came after the discovery of fullerenes, with C_{60} being the dominant species. In 1985, Harry Kroto and Richard Smalley and coworkers were studying the vaporization of graphite when they discovered this stable, ordered formation of carbon. Previously, graphite and diamond were the only structures carbon was known to form. Conducting research on C_{60} proved to be difficult at this point, because there was no known method of producing it in bulk. This problem was remedied with the work of Wolfgang Krätschmer and Donald Huffman and colleagues, who published their results in 1990. A carbon arc could be used to vaporize graphite within a chamber of helium. The soot that got deposited on the walls of the chamber during the vaporization contained

C_{60} in large enough amounts that they could now be studied. More importantly, this arc vaporization process was simple enough that any lab could perform it.[4]

After this Krätschmer-Huffman paper, Iijima began studying the soot for possible other carbon formations and found that most of the soot off the chamber wall was amorphous and not stable carbon structures. He then looked at the deposit formed on the graphite cathode, and it was here that he discovered the nanotube structures.

1.1.1 Properties

Carbon nanotubes can be thought of as a rolled-up sheet of graphite, capped with half a C_{60} molecule on each end. They can be multi-walled or single-walled. A single-walled carbon nanotube (SWNT) has a diameter around 1nm, while a multi-walled nanotube (MWNT) can have an outer diameter ranging from 2.5nm to 30nm.[4]

Carbon nanotubes can be conducting, semi-conducting, superconducting, and insulating. Some nanotubes appear to exhibit ballistic conduction along the tube, which is a characteristic of a quantum wire.[4] Ballistic conduction or transport is when electrons are able to flow without colliding into impurities or being scattered by phonons. The electrons are not slowed down, and energy is not lost in the form of heat; essentially, there is resistance free conduction along the tube. While ballistic conduction occurs only in certain nanotubes, generally, nanotubes conduct as well as copper, if not better.

Nanotubes also exhibit incredible tensile strength. They are comprised entirely of sp^2 hybridized bonds, which are even stronger than the sp^3 hybridized bonds of diamond. A MWNT was measured to have a tensile strength of 63GPa in 2000.[16] This is an order of magnitude higher than the tensile strength of steel, 1.2GPa. Nanotubes have low density, making their tensile strength appear even more impressive. Their Young's modulus is around 1000GPa[2], which is about 5 times greater than that of steel. In compression, nanotubes do not do well and tend to buckle.

6
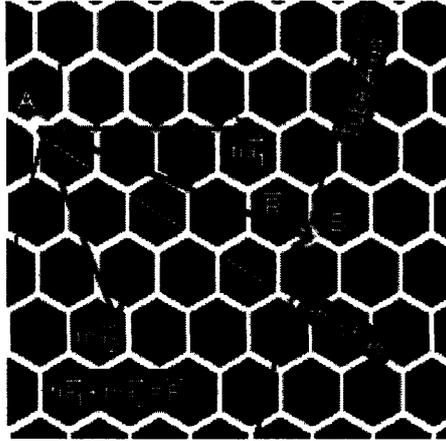
Figure 1.1: Schematic showing the vector notation used for differentiating carbon nanotubes. [1]

1.1.2 Structure notation

The properties of a nanotubes depend greatly on the chirality, or twist, of the nanotube. A schematic of how this chirality is determined can be found in Figure 1.1.

Every carbon atom on the hexagonal lattice can be represented as a sum of two vectors $\vec{a_1}$ and $\vec{a_2}$. Forming a nanotube can be thought of as putting atom A in the same location as atom B, by rolling the graphene along vector $\vec{R}$. Vector $\vec{R}$ is represented by the following:

$$\vec{R} = n\vec{a_1} + m\vec{a_2} \tag{1.1}$$

The chirality and size of a nanotube depend on the values of the coefficents n and m in Equation 1.1. They are also used in the naming of a nanotube. For example, a vector with the coefficents of n=7 and m-4 would yield a (7,4) nanotube. In general, if $\frac{n-m}{3}$ is an integer, that nanotube is metallic; therefore, about a third of all nanotubes are metallic.

There are two special kinds of CNTs, armchair and zigzag, shown in Figure 1.2. Armchair CNTs are (n,n) CNTs, while zigzag CNTs are $(n,0)$. Figure 1.3 shows the vector $\vec{R}$ for a zigzag or armchair nanotube and how the resulting tube would have the carbons in a zigzag

7
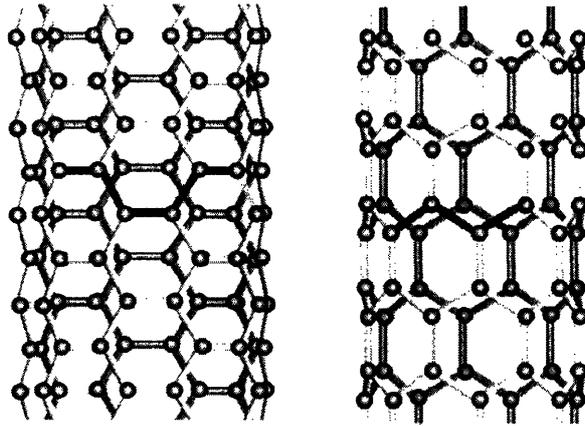
Figure 1.2: Armchair (left) and zigzag (right) nanotubes. The red outlines the armchair and zigzag patterns going around the tube. [14]
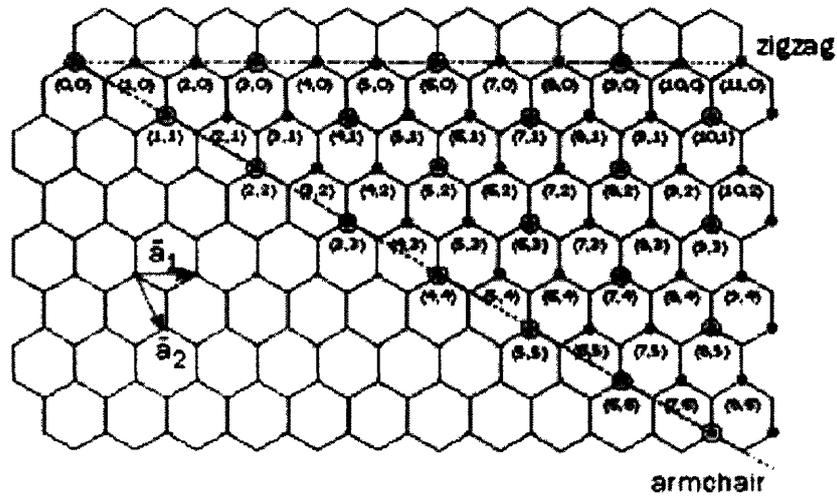
Figure 1.3: Schematic showing some of the different possible (n, m) nanotubes that can be rolled. The red vectors show the vector $\vec{R}$ that will produce a zigzag or armchair nanotube. All of the nanotubes formed from rolling along any other vector $\vec{R}$ will be chiral. The blue and green circles denote where the green circle labeled (0,0) would be superimposed in order to get that particular nanotube.[15]

8
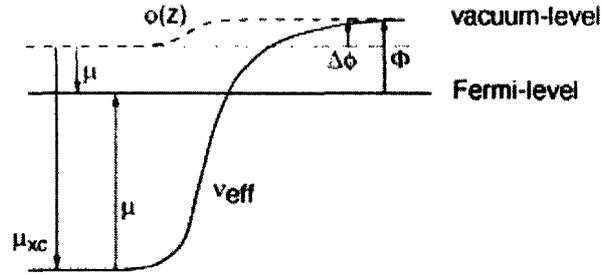
Figure 1.4: Illustration of the work function definition.[5]

or armchair pattern encircling. All other nanotubes are called chiral tubes. They are created by rolling the graphene along any vector in between the two red vectors in Figure 1.3.

1.2 Work functions

The work function is the minimum energy necessary to pull an electron at the Fermi level to a point an infinite distance away outside the surface (a vacuum). It is the minimum energy necessary to free the electron from the surface of a solid. The work function is defined for an infinitely extended crystal plane. This is different from ionization energy, which is defined for a single atom or molecule. The fermi level, or fermi energy, is defined as the smallest possible increase in energy when one electron is added to the system.

A precise knowledge of the electronic structure at a CNT/metal junction is necessary for optimal application of CNTs. In particular, the work function is an important parameter to consider when a junction with a metal is involved. It is a useful value to know for many electronic device applications, especially for CNTs used as field emission devices, such as diodes and transistors. It has been said that potential barriers at a CNT/metal interface can determine the performance of such field emission transistors.

9

1.3 Scope of this study

In this particular study, the work functions of various functionalized SWNTs are calculated. All of the nanotubes studied were (5,0) and (5,5). Work functions were calculated for pristine (5,0) and (5,5) SWNTs, fully hydrogenated (5,0) and (5,5) SWNTs, two different configurations of a (5,5) SWNT functionalized with two hydrogens, and a (5,5) SWNT functionalized with an aminophenyl group. Figures 3.1 - 3.5 show models of the nanotubes studied. The method used to calculate these work functions is discussed later in chapter 3.

Chapter 2

Background

A number of theoretical and experimental studies have been done on work functions of different CNTs. Their unique mechanical and electrical properties make them attractive candidates for a number of small-scale electronic applications. Therefore, studying the electrical properties of CNTs and the ways in which these properties change are areas of interest.

2.1 Theoretical

Given their structure, CNTs are cited as an excellent material for making field emission displays.[3] The work function is a value of interest with any field emission device. While the work function is known for elemental materials, the ways in which it changes with different CNTs are lesser known. In general, the changes in electronic structures of different nanotubes have yet to be studied. Bin Shan and Kyeongjae Cho at Stanford University conducted a first principle study of work functions of different sized SWNTs.[10] They divided the nanotubes into two categories based on diameter (D), class I $(D > 1\text{nm})$ and class II $(D < 1\text{nm})$. The work function was calculated as the Fermi level energy subtracted from the vacuum level energy. For semi-conducting nanotubes, the Fermi level was placed at the midgap.

They observed that the work functions in class I did not change depending on diameter or chirality. Work functions of nanotubes in class II showed great dependence on diameter and chirality. Within class II, they also noted that for $n < 6$, the nanotube became metallic due to curvature effects. This is visible in the band structure of a $(n,0)$ nanotube where $n < 6$. Table 2.1 shows the values they found for (5,0) and (5,5) SWNTs. [10]

Table 2.1: Values of nanotube work functions

System	Reference	Work Function(eV)
SWNT(5,0)	[10]	5.30
SWNT(5,0)	[9]	5.10
SWNT(5,5)	[10]	4.65
SWNT(5,5)	[18]	4.68
SWNT(5,5)	[9]	4.63

Shan and Cho conducted another study on the work functions of double-walled CNTs (DWNTs). [9] While similar to SWNTs, DWNTs are stiffer and more thermally stable. This makes them potentially more interesting in the use of field emission devices. DWNTs also have the unique property where the inner tube is protected by the outer tube. As expected, the inner tubes of these DWNTs have high surface curvature and work functions that vary greatly. It is known that having an SWNT with molecules such as C_{60} encapsulated inside, changes the electronic properties of the nanotube. However, the effect of encapsulating nanotubes on the work function is unknown.

They found that the work function varied up to 0.5 eV for DWNTs that had outer nanotubes of the same diameter. This variation is correlated with the type of inner nanotube that is encapsulated in the DWNT. The energetics of altering the spacing between the inner tube and outer tube were also studied, by fixing the inner nanotube and changing the diameter of the outer tube. They found that certain pairs of inner and outer tube diameters were most energetically favorable.

Another study done by Zhao et $al.$ at UNC Chapel Hill looked at work functions of

pristine and alkali-metal intercalated CNTs and bundles.[18] The work functions of alkali-metal intercalated nanotubes is of great interest because nanoscale electronics have been built based on these doped CNTs. They observed the changes in work function as different metals at different concentrations were intercalated. Contrary to Shan and Cho, they used the energy of the highest occupied molecular orbital for all tubes (including semi-conducting) when calculating the work function. They found that the work functions of metallic CNTs were somewhat dependent on the diameter. For aliki-metal intercalated nanotubes and bundles, the work function decreased significantly and the electronic states around the Fermi level changed as well. The work function decreased more as the concentration of metal dopant increased.

2.2 Experimental

Gao *et al.* studied the work function at the tips of multiwalled carbon nanotubes. The work function at the tip of the nanotube is of particular interest, because this is where most of the electrons are emitted. Gao and coworkers synthesized MWNTs and work functions of individual nanotube tips were measured using an *in situ* transmission electron microscope technique. They found that about 75% of the nanotube tips had work functions ~0.2-0.4 eV lower than that of carbon. The other 25% nanotubes were likely to be semi-conducting tubes and had work functions ~0.6 eV higher than that of carbon.

Another experimental study of work functions was done using an open counter photo-electron emission method (PEEM). [11] PEEM is a relatively easy and precise technique of measuring work functions directly. In this study, a lamp with photon energy of 3.4-6.2 eV was shined on the surface.[11] Suzuki and coworkers conducted another work function study using PEEM and viewed the work functions from images of secondary electrons with a kinetic energy of 0.7 eV. [13] They studied 93 CNTs with diameters ranging from 1-3 nm.

Most of the SWNTs they studied had work functions that fell within a range of 0.2 eV, indicating there was not a strong dependence on size and chirality. However, the work functions split into two groups, suggesting there is a difference between work functions of metallic and semi-conducting CNTs, if not a large difference. These results contradicted previous studies that indicated that work functions differed depending on size and chirality.

Ultraviolet photoemission spectroscopy (UPS) is another common technique used to measure work functions of CNTs. One advantage of UPS is that it allows one to study electronic structures in a wide energy range. Suzuki *et al.* experimentally studied the electronic structures and work functions of pristine and Cs-intercalated SWNT bundles using UPS. [12] They observed that the electronic structure differences between SWNTs and MWNTs depended mostly on tube diameters. The work functions of SWNTs were found to be slightly larger relative to graphite, while MWNTs had work functions of 0.1-0.2 eV lower. They measured the work function of the SWNT bundles as 4.8 eV, which decreased significantly to 2.4 eV with Cs-intercalation. The lowering of the work function of the Cs-intercalated nanotube bundles is likely an intrinsic bulk property and not merely Cs atoms remaining on the bundle surface. These results match the theoretical results from the study by Zhao *et al.* mentioned above. [18] Doping with Cs appears to reduce the work function of SWNTs. This study also noted the possible difference in work function between the tip of the nanotube versus the side, making it uncertain whether the work function of SWNTs can yet be directly correlated to their field emission properties.

A study by Zhang *et al.* looked at the effect of hydrogenation of SWNTs. [17] The interactions between molecules and CNTs are important to understand in order to use CNTs effectively in future applications. Zhang *et al.* studied the covalent reaction between hydrogen and SWNTs. This is distinct from weak adsorption of molecular hydrogen, which has been studied. Hydrogenation of SWNTs by atomic hydrogen or hydrogen plasma reaches an atomic coverage of up to ~65%. This was a systematic study of the covalent reactions

between hydrogen and SWNTs and observed the electrical properties of these hydrogenated SWNTs among other properties. Over 100 SWNTs were exposed to hydrogen radicals for 3 minutes and a height increase of $3\pm \sim 1$ Åwas observed with atomic force microscopy. This added height was attributed to the covalently bonded hydrogen (~ 1 Å) and the deformation and relaxation of the CNT walls from the addition of hydrogens. Systematic study of the hydrogenated CNTs showed significance decrease in conduction from the pristine nanotubes. This study attributed this decreased conduction to the change from sp^2 hydridized bonds of the carbon network to sp^3 bonds formed with hydrogenation. This change in bonds led to a localization of π-electrons, resulting in decreased conduction. It was also suggested that hydrogenated SWNTs are more semi-conducting and have a wider band gap than its dehydrogenated counterpart. The hydrogenation was mostly reversible except when harsher plasma conditions were used, such as plasma exposure for 10 min. In these cases, permanent etching, cutting, and removal of SWNTs were observed, particularly for SWNTs of smaller diameters. This suggested that harsh enough plasma conditions could completely break down the nanotube structures with smaller diameters, leading to the formation hydrocarbon molecules. The higher curvature and strain in smaller CNTs make them more reactive to hydrocarbonation, especially when hydrogenation is done at higher temperatures. This study brings into question the stability of hydrogenating smaller nanotubes.

2.3 Motivation

Precise knowledge of the work function is critical in any application involving a CNTs/metal junction and for using CNTs in field emission devices. Understanding how the work function and electronic structures change as a result of changing a parameter of the nanotube is an important step in building devices with nanotubes. This study attempts to add information to better understand the dependencies of CNT work functions.

Chapter 3

Method

The electronic structure calculations performed in this study used a quantum mechanical method, density functional theory (DFT). All of the calculations were done using a code package PWscf, which can be found at www.quantum-espresso.org.

3.1 Electronic structure calculations

3.1.1 Density functional theory

Density functional theory is a method of studying the ground state properties of metals, semi-conductors, and insulators.[7] It describes an interacting system of fermions in terms of its density, instead of the many-bodied wave function:

$$\hat{H}\Psi = [\hat{T} + \hat{V} + \hat{U}]\Psi = [\sum_{i}^{N} -\frac{\hbar^2}{2m}\vec{\nabla}_i^2 + \sum_{i}^{N} V(\vec{r_i}) + \sum_{i<j} U(\vec{r_i}, \vec{r_j})]\Psi = E\Psi. \qquad (3.1)$$

where $\hat{H}$ is the Hamiltonian, N is the number of electrons, $\hat{U}$ is the electron-electron interaction, $\hat{V}$ is the external potential in which the electrons are moving, and $\hat{T}$ is the kinetic energy operator. The many-bodied wave function, Ψ, in Equation 3.1 is dependent on $3N$

variables for N electrons, making it practically unsolvable. In the 1960s, the possibility of doing first principles calculations of systems with more than one electron came about with the work of Hohenberg and Kohn, and Kohn and Sham.

Hohenberg-Kohn theorems. The Hohenberg-Kohn (HK) theorems allow the description of the many-bodied wavefunction with N electrons, in terms of its electron density. It states that a mapping exists between the ground state density and the ground state many-bodied wavefunction. They proved that from a given ground state density $n_0(\vec{r})$, there exists the possibility to calculate its corresponding ground state wavefunction $\Psi_0(\vec{r_1}, ..., \vec{r_N})$, by reversing the relation in the particle density $n(\vec{r})$ given by:

$$n(\vec{r}) = N \int d^3r_2 \int d^3r_3 ... \int d^3r_N \Psi^*(\vec{r}, \vec{r_2}, ..., \vec{r_N}) \Psi(\vec{r}, \vec{r_2}, ..., \vec{r_N}). \tag{3.2}$$

The electronic density is dependent on three variables, no matter how large the system, as opposed to the many-bodied wavefunction which is dependent on $3N$ variables for N electrons. The mapping itself is done through the Kohn-Sham equations, discussed below. The HK theorems also proves that this ground state electron density does give the minimum electronic energy of the system.

Kohn-Sham. The Kohn-Sham equations map the relationship between the ground state density of a system and its ground state wavefunction. The equations are derived by starting with the ground state energy as a functional of the charge density, given by

$$E[\rho(r)] = T[\rho(r)] + \int \rho(r)\nu(r)dr + E_{ee} \tag{3.3}$$

where $T[\rho(r)]$ is the kinetic energy, $\int \rho(r)\nu(r)dr$, and E_{ee} is the electron-electron interaction.

$$E_{ee}[\rho(r)] = \frac{1}{2} \int \frac{\rho(r)\rho(r')}{|r - r'|} dr dr' + E_{xc}[\rho(rho)] \tag{3.4}$$

In Equation 3.4, the first part of the right side of the equation is the electron-electron electrostatic interaction and the second part is the exchange-correlation energy. The Kohn-Sham equations can represent all of the above terms exactly in terms of the electronic density, except for the exchange-correlation energy.

Exchange-correlation potential. The exchange-correlation potential describes the effects of the coulomb interactions between the electrons. Coulombic interactions involve the energy change that occurs when the wavefunctions of two or more fermions overlap and the potential from two interacting fermions. DFT approximates this potential with several different methods, the simplest one being the local-density approximation (LDA) suggested by Kohn and Sham. Unless the exact exchange-correlation potential is known, DFT cannot solve the many-bodied wavefunction exactly and can only approximate it as well as exchange-correlation potential is approximated.

3.1.2 PWscf

This study used a code package PWsf, Plane-Wave Self-Consistent Field, available as part of quantum-espresso.[8] It uses a plane-wave basis set and pseudopotentials to perform the electronic structure calculations. Bash shell scripts were written to submit jobs on the computer cluster to perform the calculations.[1] These scripts contained the necessary information to generate PWscf input files. Electronic structure calculations were done on the geometries described in a unit cell (provided by the PWscf input file), which is repeated infinitely along the x, y, and z axes. The unit cell used for all the nanotubes was a simple tetragonal lattice pictured in Figure 3.6. Figure 3.7 shows an example of a geometry that was described within a unit cell, and the repetition of that unit cell along the z-axis is shown in Figure 3.8.

For the pristine CNTs, each unit cell contained 20 carbon atoms, and 12 k-points were

---

[1] The electronic structure calculations were performed on a linux cluster at the Institute for Soldier Nanotechnology High Performance Computing Center at MIT.
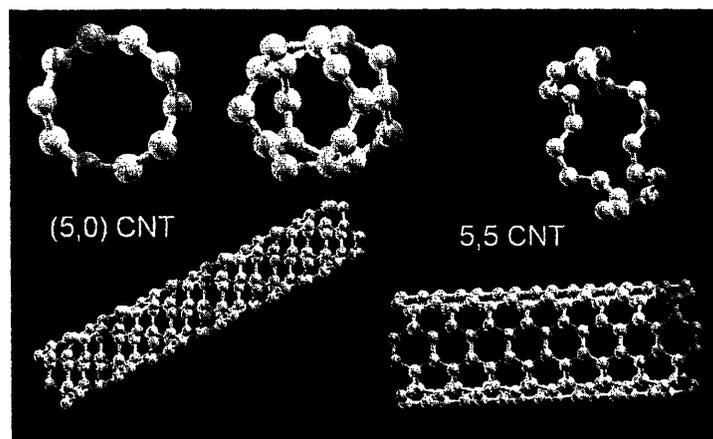
Figure 3.1: Models of the pristine (5,0) and (5,5) SWNTs.
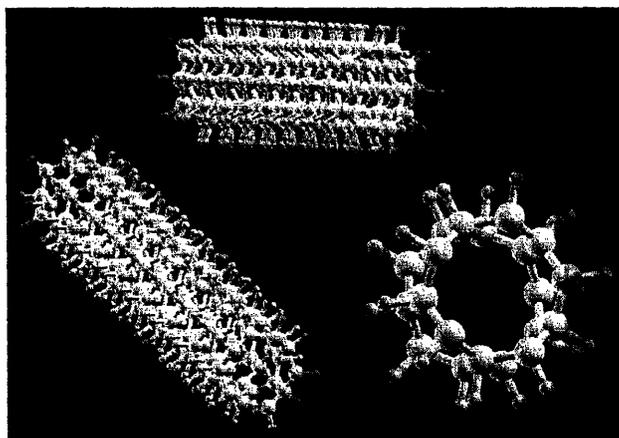
Figure 3.2: Models of the fully hydrogenated (5,0) SWNT.
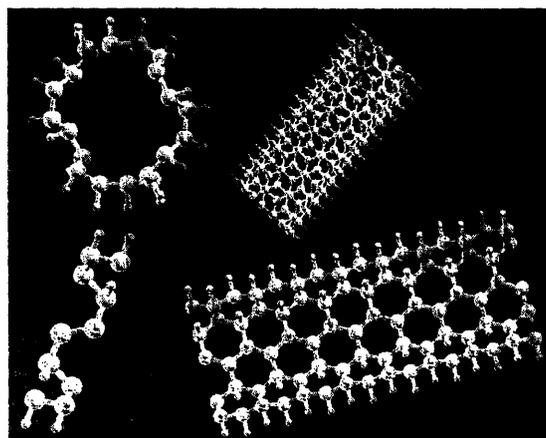
Figure 3.3: Models of the fully hydrogenated (5.5) SWNT.

19
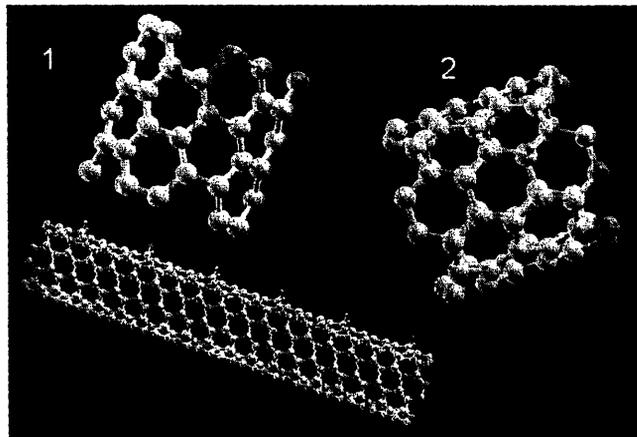
Figure 3.4: Models of the two different configurations of a (5,5) SWNT functionalized with two hydrogens. Throughout this study, these two functionalized nanotubes will be differentiated as configurations 1 and 2.
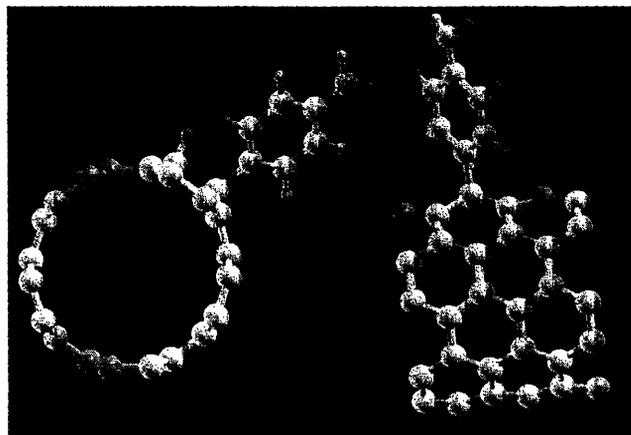
Figure 3.5: Model of (5,5) SWNT functionalized with an aminophenyl group.
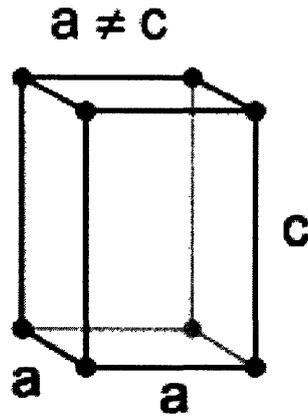
Figure 3.6: Simple tetagonal lattice. Lattice constants are a and c, where $a{\neq}c$.[6]

used. The fully hydrogenated CNTs contained 40 atoms each: 20 carbons and 20 hydrogens. 12 k-points were used for the calculations. The two CNTs functionalized with 2 hydrogens contained 62 atoms each: 60 carbons and 2 hydrogens. It was necessary to use 60 carbons to form 3 stacked rings, instead of 1 ring of 20 carbons, in order for stability in the structure. The unit cell was also made three times as long, in order to accommodate the added rings. The increase in the number of atoms and the asymmetry introduced made the calculations much more expensive, so 4 k-points were used for these two nanotubes. This was also the case for the SWNT functionalized with the aminophenyl group; the nanotube was described as a system of 60 carbons, and 4 k-points were used. Figures 3.1 - 3.5 show the geometries of the nanotubes described within the unit cells, in addition to the unit cells repeated several times along the z-axis.

For the (5,0) pristine and fully hydrogenated CNTs, $a = 31$, and $c = \frac{3cc}{a}$ where $cc = 2.685$, the carbon-carbon bond length. The pristine and fully hydrogenated (5,5) CNTs had unit cells where $a = 36$ and c was given by $\frac{\sqrt{3}cc}{a}$. The (5,5) CNTs that were hydrogenated with 2 hydrogens and an aminophenyl group had unit cells three times as long to fit the stack of 3 rings, so $c = \frac{3\sqrt{3}cc}{a}$.

Figure 3.7: Geometry of a (5,0) CNT described as a 20-carbon ring within a unit cell. All of the nanotubes were described as rings, which could be repeated to form a tube (See Figures 3.1-3.4). Calculations were performed on the geometries described within a unit cell.
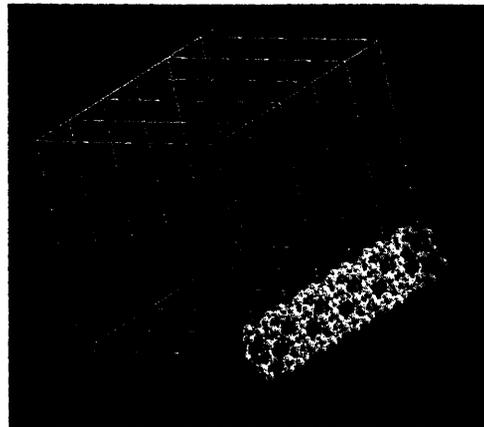
Figure 3.8: Unit cell of the (5,0) CNT repeated along the z-axis. The white outlines denote the outline of the unit cell. The empty space is necessary, because the unit cell can be repeated along the x, y, and z axes. There must be enough vacuum space around the ring so they do not interact with each other when repeated along the x and y axes.

Plane-wave basis set. The plane-wave basis set is a discrete set of plane waves that describe the electronic wavefunction at a given k-point. Using a plane-wave basis set to express the wavefunction offers a number of advantages including the systematic increase in accuracy by increasing cutoff energy (i.e. adding more plane waves) and efficient transforms to fourier space.

Pseudopotential The pseudopotential approximation attempts to replace the effect of the core electrons and nucleus with an effective potential. Using an approximation is possible, because the valence electrons play a much greater role in the properties of solids than the tightly bound core electrons. For example, only the valence electrons are involved in chemical bonding.

3.1.3 XCrysDen

XCrysDen, available at `www.xcrysden.org`, is an application for visualizing crystalline and molecular structures. All of the nanotubes studied were viewed using XCrysDen to ensure that their geometries were described correctly. It was also used to check that the unit cell was described as the correct size such that repeating it would give the desired nanotube structure.

3.1.4 Geometry optimization

The nanotube geometries were described by cartesian coordinates which described the position of each of the atoms comprising the nanotube. These geometries were optimized with PWscf; throughout the calculation, PWscf calculated the directional forces acting on each atom and propagated the position of the atom accordingly. The structure was considered relaxed when the forces on the atoms were close to 0 eV/au and the positions of the atoms were changing negligibly. Generally, the forces felt on each atom was on the order of thousandths of a eV/au once the optimal geometry had been found. The new coordinates generated by PWscf were written to an output file, along with the Fermi level for the system. For semi-conducting nanotubes, the energy of the highest occupied molecular orbital (HOMO) was used as the Fermi level when calculating the work function.

3.2 Calculating the work function

These relaxed coordinates were put into another script file to run calculations that generated the electrostatic potential in the unit cell of the nanotube. The potentials were found for different points in the unit cell and written to an output file. The planar average of the potentials were plotted over one axis.

From this plot, the vacuum level was found. The potential at the cell boundary was the
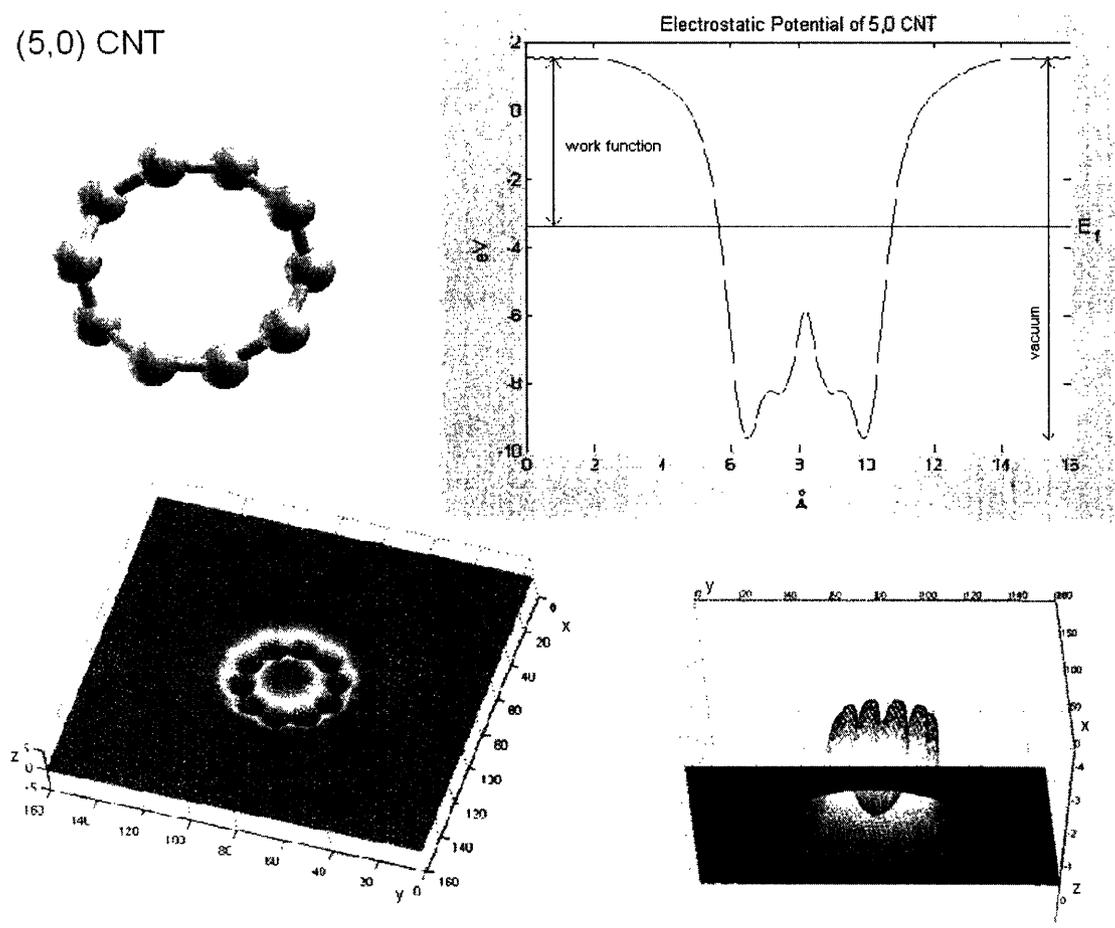
Figure 3.9: The process of calculating the work function for a pristine (5,0) CNT. The 20-carbon ring was described in the unit cell, and the geometry was optimized. Using the optimal coordinates, the electrostatic potential in the unit cell was calculated. The two lower plots show a plot of the potential averaged over the z-axis of the cell. The dark red region is the vacuum level of the cell. It is possible to see in these plots how the nanotube was positioned in the unit cell. Projecting this particular 20-carbon ring onto the xy-plane gives a shape of a 10-carbon ring, as seen in the model of the ring in the upper left. The plot in the upper right shows the potential averaged and projected onto the x-axis. From this plot, the vacuum level was found as the potential value sufficiently far from the nanotube. The work function was determined by subtracting the Fermi level from the vacuum level.

24

vacuum level used to calculate the work function, and this was the first potential value from the planar average. Subtracting this vacuum from the fermi level got the work function for that particular nanotube. Figure 3.9 illustrates the method described above.

After calculating the work function, more calculations were done to create band structures. The coordinates of the relaxed geometries were put into another shell script that ran band structure calculations. For all of the band structure calculations for the nanotubes, 100 k-points were used. From these plots, it was possible to see how the band gap of the nanotube had changed from the functionalizations.

Chapter 4

Results and Discussion

4.1 Work functions

The work functions of the nanotubes decreased with functionalization. Table 4.1 summarizes the work functions calculated in this study, in addition to the Fermi levels and vacuum levels found. These work functions were calculated by obtaining the Fermi level, or the HOMO for semi-conducting tubes, from the output files of the relaxation calculations. The vacuum level was obtained from the plots shown in Figures 4.1 - 4.7, which are the planar average of the electrostatic potential in the unit cell, plotted as a function of the x-axis of the cell. The vacuum level was taken as the potential at the cell boundary.

Table 4.1: Calculations of Work Functions

System	Fermi Level(eV)	Vacuum (eV)	Work Function(eV)
pristine SWNT(5,0)	-3.30	1.55	4.85
fully hydrogenated SWNT(5,0)	-1.10	1.55	2.65
pristine SWNT(5,5)	-1.98	2.02	4.00
fully hydrogenated SWNT(5,5)	-1.76	2.02	3.78
SWNT(5,5) + 2H (1)	-1.93	1.95	3.88
SWNT(5,5) + 2H (2)	-1.86	2.04	3.90
SWNT(5,5) + Aminophenyl group	-1.53	2.21	3.74
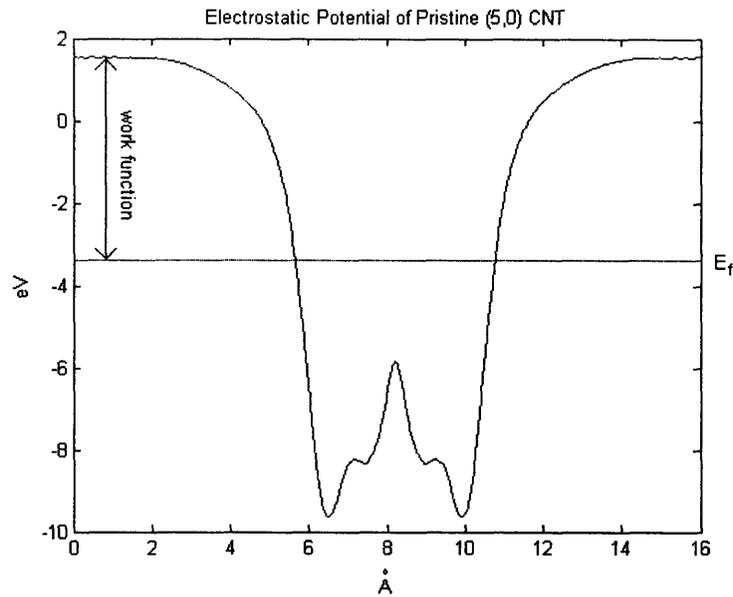
Figure 4.1: Planar average of the electrostatic potential along the x-axis for the pristine (5,0) CNT.

The calculated work functions for the pristine (5,0) and (5,5) SWNTs differed from values found in previous studies. One possible reason for the discrepancies is the exchange correlation potential. The generalized gradient approximation (GGA) functional PBE was used in this study, while in the other studies the local density approximation (LDA) was used. [9, 10, 18] Also, this study used 12 k-points when performing the calculations, while other theoretical studies used 30 and 40 k-points. Other than these two factors, it is not entirely clear why different work functions were found. In both the pristine (5,0) and (5,5) SWNTs, the work functions found in this study were lower than those found in previous studies.

The lowering of the work function with the addition of side groups is consistent with the study done by Suzuki *et al.* and Zhao *et al.* where they calculated the work functions of Cs-intercalated CNTs and bundles. They observed a significant decrease in the work function with Cs intercalation, which is consistent with the lowering of the work functions

27
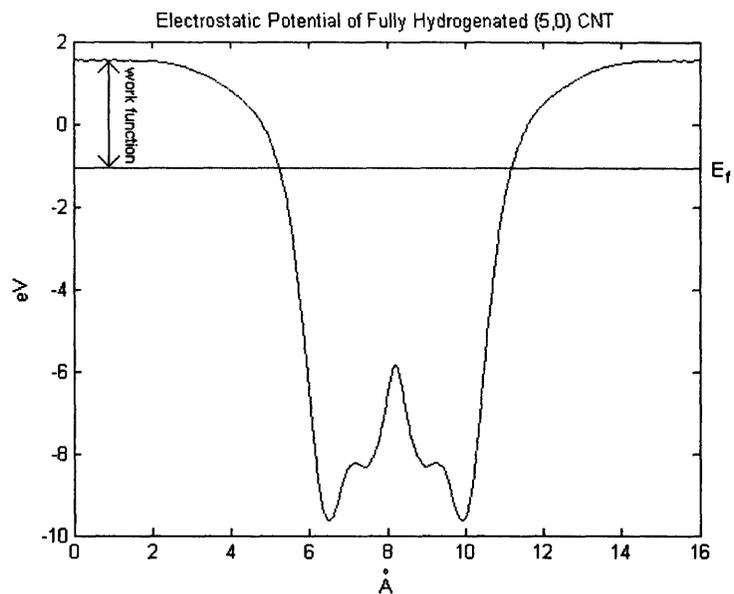
Figure 4.2: Planar average of the electrostatic potential along the x-axis for the fully hydrogenated (5,0) CNT.
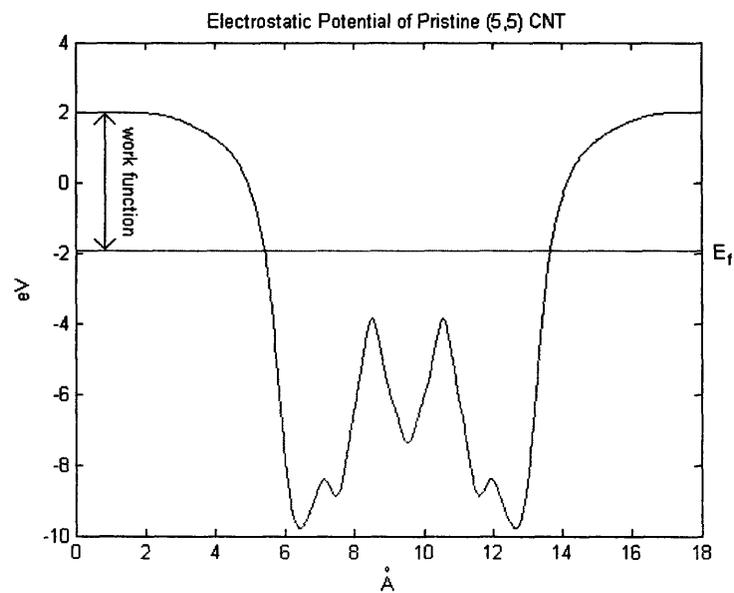
Figure 4.3: Planar average of the electrostatic potential along the x-axis for the pristine (5,5) CNT.
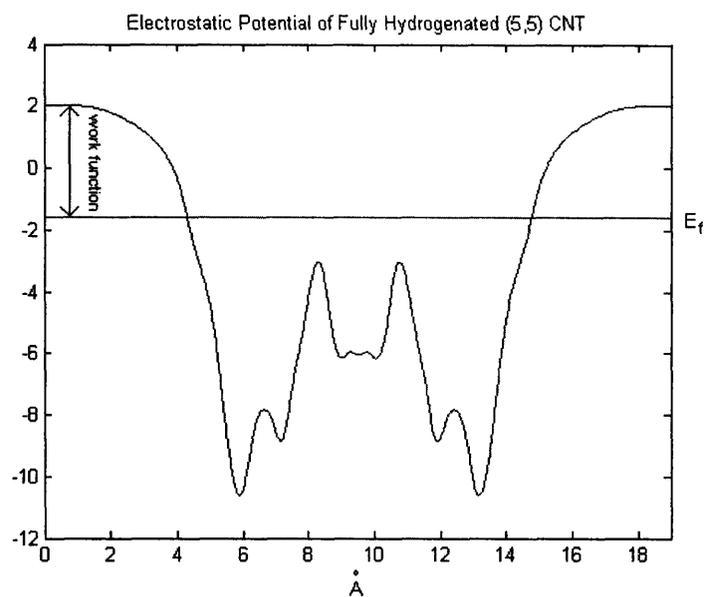
Figure 4.4: Planar average of the electrostatic potential along the x-axis for the fully hydrogenated (5,5) CNT.
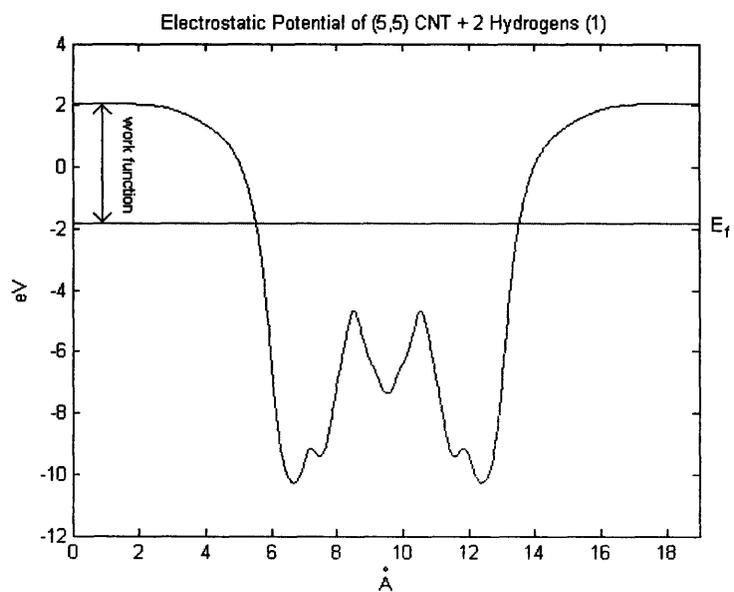
Figure 4.5: Planar average of the electrostatic potential along the x-axis for the pristine (5,5) CNT functionalized with 2 hydrogens (Configuration 1).
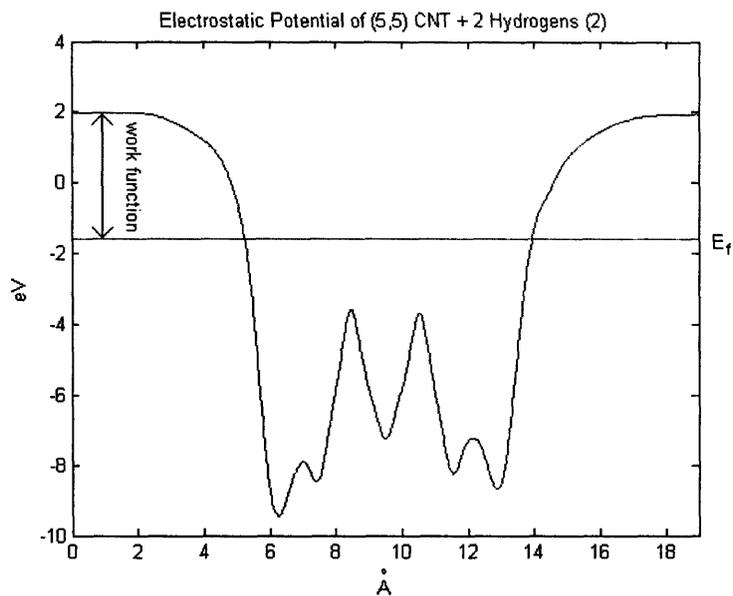
Figure 4.6: Planar average of the electrostatic potential along the x-axis for the pristine (5,5) CNT functionalized with 2 hydrogens (Configuration 2).
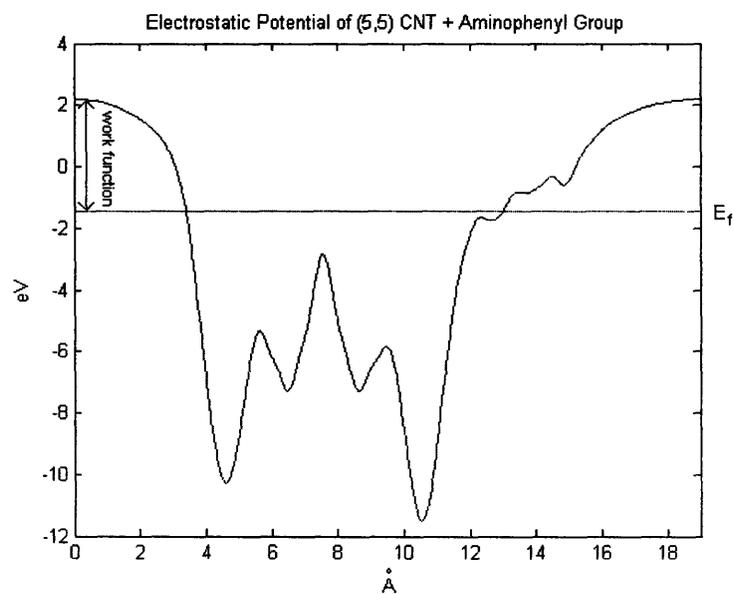
Figure 4.7: Planar average of the electrostatic potential along the x-axis for the (5,5) CNT functionalized with an aminophenyl group.
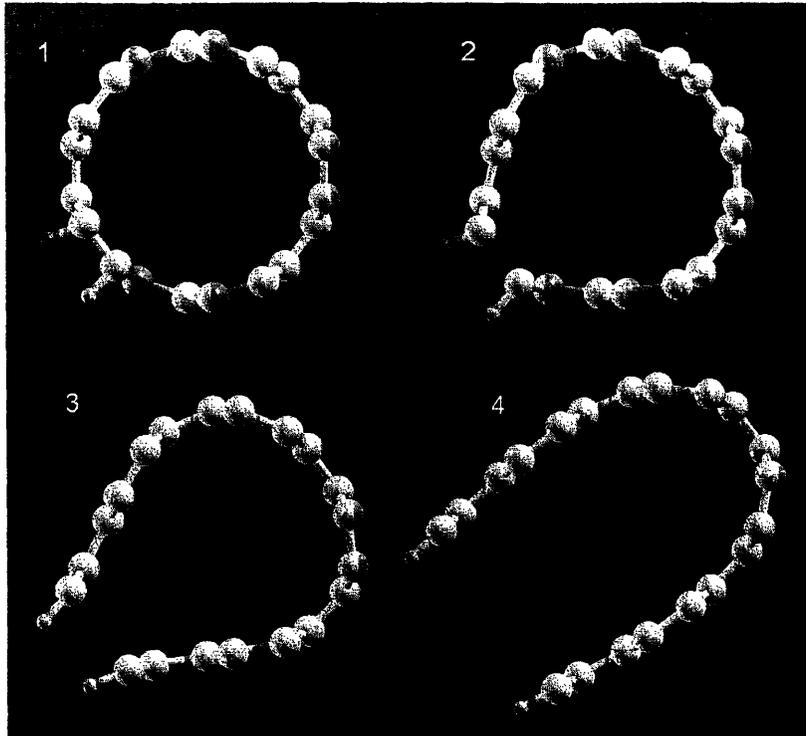
Figure 4.8: Relaxation of a (5,5) CNT functionalized with 2 hydrogens. The structure was unstable when the nanotube was defined with only 20 carbons. 60 carbons were necessary to have an energetically stable structure when functionalizing with two hydrogens.

observed in this study. The study by Zhao *et al.* also observed a correlation between the lowering of the work function and concentration of the metal. The more metal that was intercalated with the nanotube, the lower the work function became. These observations are also consistent with the results of this study; the nanotubes with greater functionalization experienced greater lowering of the work function from its pristine counterpart.

The work function of the (5,5) SWNT decreased more dramatically when fully hydrogenated, than when it was functionalized with just 2 hydrogens. The work functions of the two configurations of functionalization by 2 hydrogens were different from each other by only 0.02 eV. It appears as though the placement of the hydrogens does not have an effect the work function, although the concentration of hydrogen does.

31
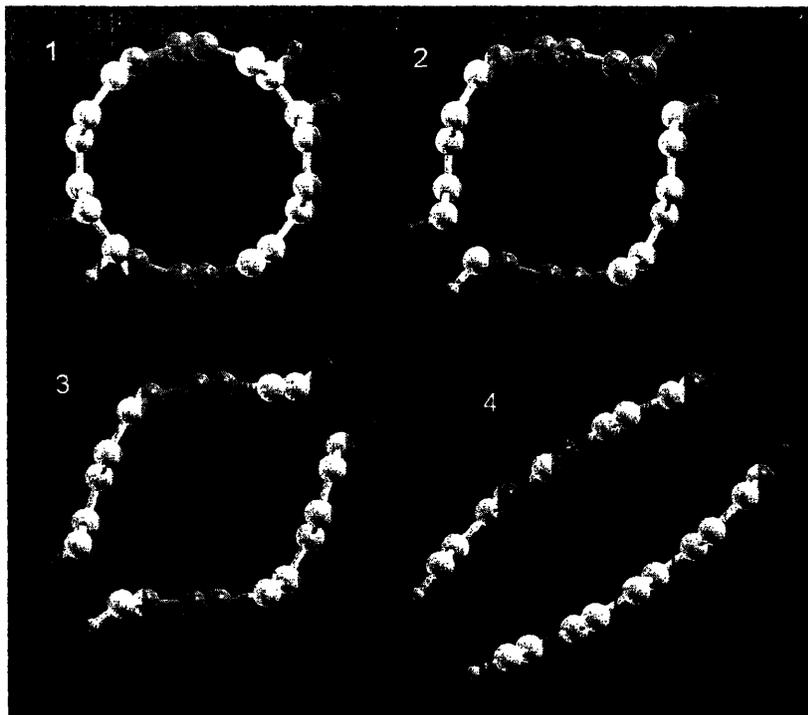
Figure 4.9: Relaxation of a (5,5) CNT functionalized with 4 hydrogens. The structure was unstable when the nanotube was defined with only 20 carbons. Relaxing this nanotube resulted in its splitting.

The instability of smaller nanotubes during hydrogenation discussed in the study by Zhang *et al.* was also observed. Smaller nanotubes experience higher curvature and strain, and the addition of hydrogens can induce cutting of the nanotube. Originally, the nanotubes functionalized by 2 hydrogens were described by a single ring, or 20 carbons atoms. The hydrogens caused the nanotube to break open when it was relaxed. The 20 carbon ring was not stable enough for hydrogenation by 2 hydrogens and the ring opened up, as seen in Figure 4.8. The ring split in between the two hydrogens, indicating that the (5,5) nanotube structure with hydrogens along the axis of the tube is not energetically stable. The same held true with a 20 carbon ring of a (5,5) CNT that was functionalized with 4 hydrogens. As seen in Figure 4.9. the nanotube broke as it was relaxed. Again, it broke in between the location of the hydrogens: since such a location exists twice in this structure, the nanotube

32

broke in two places. It is possible that an actual nanotube would have split down its length due to the high curvature and strain.

The fully hydrogenated (5,0) and (5,5) nanotubes did not break, because the structures were fully symmetric. All of the bonds are sp^3 hybridized in these two SWNTs, and thus the stresses on the nanotube are uniform. The energetics of these systems did not lead to cutting of the nanotube. However, it is unclear whether it is possible to fully hydrogenate such small nanotubes. Experimental results show that nanotubes that are hydrogenated form atomic coverage of ~65%. [17] It appears as though nanotubes have not been hydrogenated 100%, such as the ones studied theoretically here. Harsher plasma conditions cannot be used for hydrogenation, because it may lead to cutting of the nanotube, particularly in small CNTs. [17] It may not currently be possible to hydrogenate a nanotube with 100% coverage.

4.2 Band structures

The band structures of all the nanotubes were also studied. As expected, the pristine (5,0) SWNT had no band gap (Figure 4.10). Although a (5,0) SWNT should be semi-conducting according to the $\frac{n-m}{3}$ rule, the nanotube is actually metallic because of curvature effects. If a $(n,0)$ CNT has $n < 6$, that nanotube is metallic. [10] In the band structures of these nanotubes, the singly degenerate π band is lowered below the valence band top. This downward shift of the singly degenerate state is induced by high curvature.

The band structures of interest are the pristine and fully hydrogenated (5,5) SWNTs, Figure 4.11. The bands cross in the band structure of the pristine (5,5) SWNT, so this nanotube is metallic. However, full hydrogenation opened a gap of 2.15 eV in the band structure, indicating that the nanotube became semi-conducting, or at least, more semi-conducting. This reduction of metallic nature is consistent with the study by Zhang $et\ al.$, where they consistently observed a significant decrease in conduction after H-plasma exposure. The
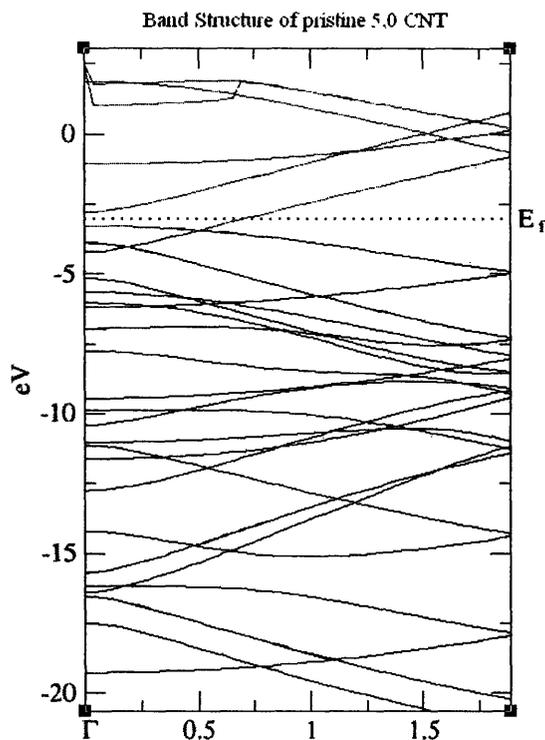
Figure 4.10: Band structure for the pristine (5,0) CNT.

decrease in conductance after hydrogenation can be attributed to the change of hybridized bonds. CNTs are comprised of sp^2 hybridized bonds, which become sp^3 when hydrogenated. This leads to the localization of π-electrons, resulting in decreased conductivity.

The opening of a small band gap of 0.43 eV was also observed in the band structure of configuration 1 of the (5,5) SWNT functionalized with 2 hydrogens, Figure 4.12. There was no band gap in configuration 2, but the bands shifted and crossed in a different location from the pristine nanotube.

Table 4.2: Calculations of Work Functions using Midgap as the Fermi Level

System	HOMO(eV)	LUMO(eV)	Midgap(eV)	Work Function(eV)
fully H SWNT(5,5)	-1.7608	0.3920	-1.3688	3.39
SWNT(5,5) + 2H (1)	-1.9345	-1.8439	-1.8892	3.84

34
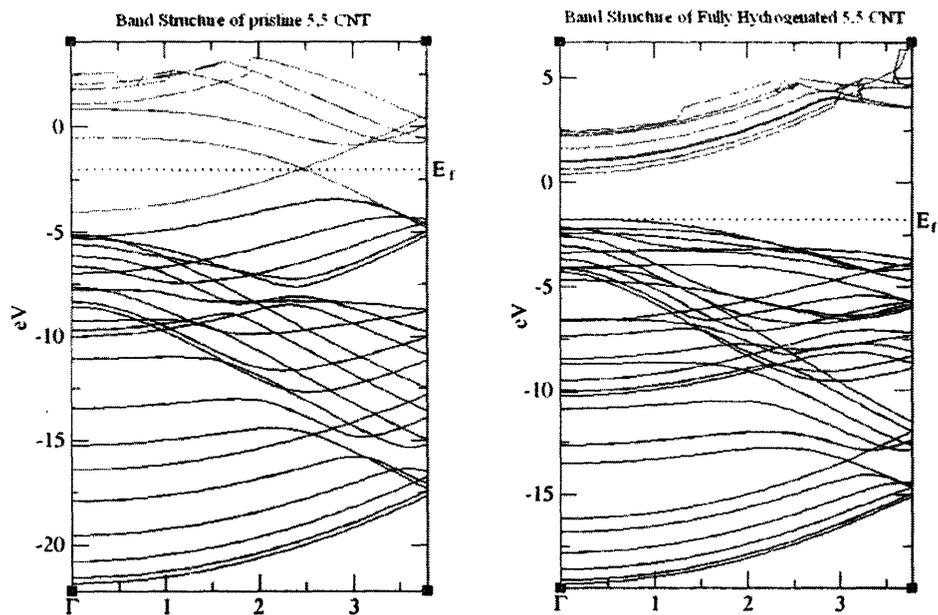
Figure 4.11: Band structures for the pristine (5,5) CNT on the left and the fully hydrogenated (5,5) CNT on the right.
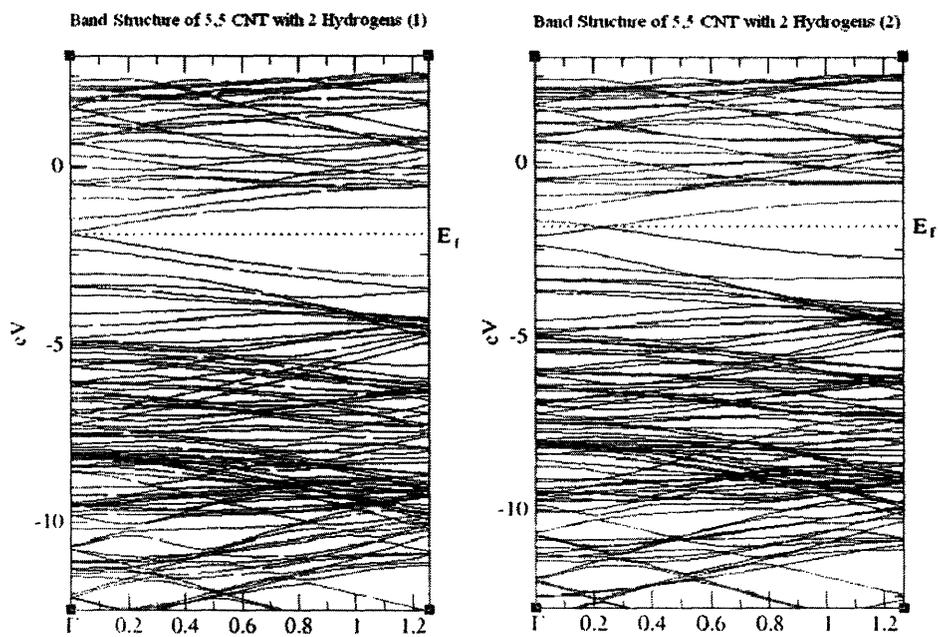
Figure 4.12: Band structures for the (5,5) CNT functionalized with 2 hydrogens. Configuration 1 on the left, and configuration 2 on the right.

For the semi-conducting CNTs, the Fermi level was taken as the energy of the highest occupied molecular orbital (HOMO). However, some studies have used the midgap level, calculated from the HOMO and the lowest unoccupied molecular orbital (LUMO), as the Fermi energy. Table 4.2 shows the work functions for the fully hydrogenated (5,5) SWNT and configuration 1 of the (5,5) SWNT functionalized with 2 hydrogens, if they were calculated using the midgap as the Fermi level, instead of the HOMO. There was a decrease in the work function, because the Fermi level used was higher when taken as the midgap. This was particularly true for the fully hydrogenated (5,5) SWNT which had a work function of 3.78 eV when using the HOMO as the Fermi level. The value of the work function of semi-conducting CNTs will be affected by the bandgap if the HOMO is used in its calculation, especially if this induced band gap is relatively large.

Chapter 5

Conclusion

A systematic study of the work functions of differently functionalized SWNTs was conducted. The work functions decreased with functionalizations. This is seen with the (5,5) SWNT with an aminophenyl group attached, which had a work function of 3.74 eV. This is in comparison to the pristine (5,5) SWNT which had a work function of 4.00 eV. The concentration of hydrogen functionalizing the nanotube affects the work function, while the locations of the hydrogens do not. With the smaller nanotubes, the high curvature and strain makes them energetically unstable to hydrogenation.

Functionalizations also affect the band structures of the nanotubes. Hydrogenated nanotubes behave more like semi-conducting materials than metallic, due to the localization of π-electrons. In this study, using the HOMO as the Fermi level in the semi-conducting nanotubes made the work function higher than when the midgap was used. The size of the bandgap also played a role in how much the work function was affected by using the HOMO as the Fermi level.

This work has shown that with functionalization, the electronic structure and properties of small SWNTs can be tailored. This control over work function in particular could be of significant importance to the design of electronic devices.

Bibliography

[1] T. A. Adams, "Physical Properties of Carbon Nanotubes",
www.pa.msu.edu/cmp/csc/ntproperties

[2] L. Forró, et al.,"Electronic and Mechanical Properties of Carbon Nanotubes"', Proceedings of Nanotube, 1999.

[3] R. Gao, Z. Pan, Z. L. Wang, "Work function at the tips of multiwalled carbon nanotubes", APL, 2001, 78, 1757-1759.

[4] P. J. F. Harris, "Carbon Nanotubes and Related Structures - New Materials for the Twenty-first Century", Cambridge University Press, Cambridge, 1999.

[5] P. Hofmann, "Work Function",
whome.phys.au.dk/~philip/q1_05/surflec/node29.html

[6] D. Mayer, "Crystal Structure",
encyclopedia.laborlawtalk.com/Image:Tetragonal.png

[7] Ohio State Univ., "Density Functional Theory",
www.physics.ohio-state.edu/~aulbur/dft.html

[8] Quanum Espresso, www.quantum-espresso.org

[9] B. Shan, K. Cho, "first principles study of work functions of double-wall carbon nanotubes", PRL, 2006, 73, 081401.

[10] B. Shan, K. Cho, "First Principles Study of Work Functions of Single Wall Carbon Nanotubes", PRL, 2005, 94, 236602.

[11] M. Shiraishi, M. Ata, "Work function of carbon nanotubes", Carbon, 2001, 39, 1913-1917.

[12] S. Suzuki, C. Bower, Y. Watanabe, O. Zhou, "Work functions and valence band states of pristine and Cs-intercalated single-walled arbon nanotube bundles", APL, 2000, 76, 4007-4009.

[13] S. Suzuki, Y. Watanabe, Y. Homma, "Work functions of individual single-walled carbon nanotubes", APL, 2004, 85, 127-129.

[14] E. Thostenson, "Tsu-Wei Chou heads interdisciplinary carbon nanotube research project", University of Delaware - UDaily, 2003, `www.udel.edu/PR/UDaily/2004/Chou-Atomic-Structureslg.jpg`

[15] Yale University, "Electronic and optical properties: carbon nanotubes", `volga.eng.yale.edu/sohrab/grouppage/CNT.html`

[16] M. F. Yu, O. Lourie, M. J. Dyer, K. Moloni, T. F. Kelly, R. S. Ruoff, "Strength and Breaking Mechanism of Multiwalled Carbon Nanotubes Under Tensile Load", Science, 2000, 287, 637-640.

[17] G. Zhang, P. Qi, X. Wang, Y. Lu, D. Mann, X. Li, H. Dai, "Hydrogenation and Hydrocarbonation and Etching of Single-Walled Carbon Nanotubes", JACS, 2006, 128, 6026-6027.

[18] J. Zhao, J. Han, J. P. Lu, "Work functions of pristine and alkali-metal intercalated carbon nanotubes and bundles", PRB, 2002, 65, 193401.